Received: 6 December 2018 | Revised: 15 March 2019 | Accepted: 20 March 2019

DOI: 10.1111/cas.14007

ORIGINAL ARTICLE

WILEY Cancer Science

Serum deprivation-response protein regulates aldehyde dehydrogenase 1 through integrin-linked kinase signaling in endometrioid carcinoma cells

Shinichiro Tahara[1] | Satoshi Nojima[1] | Kenji Ohshima[1] | Yumiko Hori[1] | Masako Kurashige[1] | Naoki Wada[1] | Yuichi Motoyama[1] | Daisuke Okuzaki[2] | Jun-ichiro Ikeda[1] | Eiichi Morii[1]

[1]Department of Pathology, Osaka University Graduate School of Medicine, Osaka, Japan

[2]Genome Information Research Center, Research Institute for Microbial Diseases, Osaka University, Osaka, Japan

Correspondence
Eiichi Morii, Department of Pathology, Osaka University Graduate School of Medicine, Osaka, Japan.
Email: morii@molpath.med.osaka-u.ac.jp

Funding information
Project MEET, Osaka University Graduate School of Medicine; The Ministry of Education, Culture, Sports, Science and Technology, Japan, Grant/Award Number: T16K086490, T17K195550, T18K070680, T18K150780, T18K150790 and T18K151220

Endometrioid carcinoma (EC) is one of the most common malignancies of the female genital system. We reported previously that aldehyde dehydrogenase 1 (ALDH1), a predominant isoform of the ALDH family in mammals and a potential marker of normal and malignant stem cells, is related to the tumorigenic potential of EC. We compared the levels of various proteins in human EC cells with high and low ALDH1 expression using shotgun proteomics and found that serum deprivation-response protein (SDPR) was preferentially expressed in cells with high ALDH1 expression. Also known as cavin-2, SDPR is a member of the cavin protein family, which is required for the formation of caveolae. Using SDPR-knockout EC cells generated using the CRISPR/Cas9 system, we revealed that SDPR was correlated with invasion, migration, epithelial-mesenchymal transition, and colony formation, as well as the expression of ALDH1. RNA sequencing showed that integrin-linked kinase (ILK) signaling is involved in the effect of SDPR on ALDH1. Immunohistochemical analysis revealed that the localization of ILK at the cell cortex was disrupted by SDPR knockout, potentially interfering with ILK signaling. Moreover, immunohistochemical analysis of clinical samples showed that SDPR is related to histological characteristics associated with invasiveness, such as poor differentiation, lymphatic invasion, and the microcystic, elongated, and fragmented histopathological pattern. This is, to our knowledge, the first report that SDPR is related to tumor progression.

KEYWORDS
aldehyde dehydrogenase 1, endometrioid carcinoma, integrin-linked kinase, microcystic, elongated and fragmented, serum deprivation-response protein

Abbreviations: ADSL, adenylsuccinate lyase; ALDH, aldehyde dehydrogenase; CRISPR, clustered regularly interspaced short palindromic repeats; EC, endometrioid carcinoma; EMT, epithelial–mesenchymal transition; EV, empty vector; HDR, homology-directed repair; ILK, integrin-linked kinase; IPA, ingenuity pathway analysis; MELF, microcystic, elongated, and fragmented; N-cadherin, neural cadherin; SDPR, serum deprivation-response protein; TGF, transforming growth factor.

This is an open access article under the terms of the Creative Commons Attribution-NonCommercial-NoDerivs License, which permits use and distribution in any medium, provided the original work is properly cited, the use is non-commercial and no modifications or adaptations are made.
© 2019 The Authors. *Cancer Science* published by John Wiley & Sons Australia, Ltd on behalf of Japanese Cancer Association.

1 | INTRODUCTION

Endometrioid carcinoma is one of the most common malignancies of the female genital system. We reported previously that ALDH1, a predominant isoform of the ALDH family in mammals and a potential marker of normal and malignant stem cells, is related to tumorigenic potential and high ALDH1 expression is an independent factor for poor prognosis in EC.[1,2] We compared the levels of several proteins in HEC-1B human EC cells with high ALDH1 expression (ALDH-hi) vs low ALDH1 expression (ALDH-lo) using shotgun proteomics. The results indicated that several proteins, such as S100A4 and ADSL, are preferentially expressed in ALDH-hi cells.[3,4] Serum deprivation-response protein is reportedly also preferentially expressed in ALDH-hi cells.[3]

Serum deprivation-response protein, also known as cavin-2, is a member of the cavin family of proteins. Like caveolin, cavin proteins are required for the formation of caveolae, which are specialized membrane invaginations essential for signal transduction.[5,6] Hansen et al[7] reported that SDPR promotes recruitment of cavin-1 to caveolae and is required for stable expression of caveolin-1 and cavin-1. Members of the cavin family could be involved in tumor suppression or oncogenesis, depending on the tumor type.[8] In the present study, we investigated the role of SDPR in EC.

S100A4 accelerates the proliferation and invasion of EC cells with high ALDH1 expression and is associated with the MELF histological pattern.[3] Adenylsuccinate lyase enhances cell proliferation, migration, and invasion by regulating the effect of the oncometabolite fumarate on killer cell lectin-like receptor C3 expression. However, depletion of S100A4 or ADSL was not found to affect the expression of ALDH1.[4] In contrast, we report here that depletion of SDPR severely attenuated ALDH1 expression. We also analyzed the mechanism underlying the effect of SDPR on ALDH1.

2 | MATERIALS AND METHODS

2.1 | Patients

We examined 126 patients undergoing surgery for EC of the uterine corpus at Osaka University Hospital (Osaka, Japan) from 1998 to 2017. Resected specimens were fixed in 10% formalin and processed for paraffin embedding. The specimens were stored at room temperature in a dark room. Specimens for evaluation were sectioned at 4 μm thickness and stained with H&E. Tumors were classified according to their histological grade (G1, G2, or G3), myometrial invasion, and lymphatic invasion. This study was approved by the Ethics Review Board of the Graduate School of Medicine, Osaka University (no. 15234).

2.2 | Immunohistochemistry

Immunohistochemical staining was undertaken using the Ventana BenchMark GX autostainer (Roche, Basel, Switzerland) according to the manufacturer's instructions. We determined the cytosol and plasma membrane staining of cancer glands as positive. Negative SDPR expression was designated when cytosol and plasma membrane staining was not present in any tumor cells. Two pathologists (ST and KO) assessed the specimens independently.

2.3 | Cell lines and sorting of the ALDH-hi cell population

The human EC cell lines HEC-1B, HEC-108, HEC-116, and SNG-M were obtained from the Health Science Research Resources Bank of Osaka, Japan. Cells were cultured in DMEM supplemented with 10% FBS (Biosera, Nuaille, France). To evaluate ALDH-hi cell populations, we used the Aldefluor Kit (Stem Cell Technologies, Vancouver, BC, Canada), according to the manufacturer's instructions. Briefly, cells were suspended in Aldefluor assay buffer containing ALDH substrate and incubated for 30 minutes at 37°C. As a negative control, each sample was treated with 50 mmol/L diethylaminobenzaldehyde, a specific ALDH inhibitor. HEC-1B and HEC-108 cells were sorted into ALDH-hi and ALDH-lo populations by flow cytometry using the FACS Aria instrument (BD Biosciences, San Jose, CA, USA).

2.4 | Generation of SDPR-knockout HEC-1B and HEC-108 cells using the CRISPR/Cas9 system

HEC-1B and HEC-108 cells were seeded onto 60 mm plates. After the cells reached 70% confluency, they were cotransfected with equal amounts of an SDPR CRISPR/Cas9 knockout plasmid and SDPR HDR plasmid (sc-406898 and sc-406898-HDR, respectively; Santa Cruz Biotechnology, Dallas, TX, USA) using Lipofectamine 2000 reagent (Thermo Fisher Scientific, Waltham, MA, USA). Next, we constructed stable SDPR-knockout (KO1 and KO2) cell lines using puromycin selection (0.25 μg/mL). Similarly, we cotransfected a control CRISPR/Cas9 plasmid (sc-418922; Santa Cruz Biotechnology) and SDPR HDR plasmid into HEC-1B and HEC-108 cells and selected stably transfected cells using puromycin to generate a stable control cell line (EV).

2.5 | Antibodies

An Ab against SDPR (HPA039325; Merck, Darmstadt, Germany) was used for immunoblotting (1:250), immunohistochemistry (1:1000), and immunofluorescence (1:500) analyses. Antibodies for immunoblotting against N-cadherin, vimentin, and snail (1:1000; EMT Antibody Sampler Kit, no. 9782), ALDH1A1 (1:1000; no. 54135), AKT (1:1000; no. 4691) and phospho-AKT (Ser473; 1:2000; no. 4060) were obtained from Cell Signaling Technology (Danvers, MA, USA). An Ab against ILK1 (no. 3862; Cell Signaling Technology) was used for immunoblotting (1:1000) and immunofluorescence (1:100) analyses. Antibodies against β-actin (1:1000; 13E5, HRP conjugate, no. 5125) and lamin A/C

(1:1000; no. 2032), as immunoblotting loading controls, were also purchased from Cell Signaling Technology.

2.6 | Immunoblotting

Cells were lysed in buffer containing 10 mmol/L HEPES, 10 mmol/L KCl, 1 mmol/L EDTA, 1 mmol/L DTT, and 0.1% Nonidet P-40. Nuclei were extracted using the NE-PER Nuclear and Cytoplasmic Extraction Reagents (Thermo Fisher Scientific) according to the vendor's protocol. Electrophoresis was carried out in 5-20% gradient SDS–polyacrylamide gels (ATTO, Tokyo, Japan), and proteins were transferred to PVDF membranes (Merck). Primary Abs were detected using an HRP-conjugated anti-rabbit IgG (H + L chain) (1:5,000; MBL, Nagoya, Japan). We quantified the results using ImageJ (https://imagej.nih.gov/ij/).

2.7 | Proliferation assay

To evaluate proliferation, cells were seeded at 1×10^5 per well in 6-well culture plates (Greiner Bio-One, Frickenhausen, Germany) and cultured for 4 days at 37°C in an atmosphere containing 5% CO_2. Cells were counted on days 2 and 4 using the Muse Cell Analyzer (Merck).

2.8 | Matrigel invasion assay

Tumor cell invasion was examined using the Corning BioCoat Matrigel Invasion Chamber (Corning Inc. Corning, NY, USA). Tumor cells were placed in the upper chamber in DMEM without FBS and incubated at 37°C for 24 hours. The lower chamber contained DMEM with 10% FBS. Invasive cells (ie, those that migrated to the lower side of the upper chamber) were stained with Diff-Quik (Sysmex, Hyogo, Japan). The number of invasive cells was counted in 5 random fields per chamber at high magnification.

2.9 | Wound-healing assay

Confluent SDPR-knockout cells (KO1 and KO2) and control cells (EV) were wounded using sterilized pipette tips and incubated in culture medium for 24 hours. The migration distance was calculated by subtracting the width of the wound at 24 hours from that at 0 hour. The migration distances of KO1 and KO2 cells are expressed as the proportion of that of the EV cells.

2.10 | Chemotaxis assay

KO1, KO2, and EV cells were seeded into μ-Slide I IbiTreat chambers (no. 80106; Ibidi, Planegg, Germany), which have reservoirs for medium on both ends. After incubation for 12 hours to allow adherence, the medium was exchanged for DMEM without FBS, and the cells were incubated for 12 hours. Subsequently, recombinant TGF-β1 (R&D Systems, Minneapolis, MN, USA) was added to the left reservoir (20 ng), and the cells were incubated for 4 hours. Next, the cells were fixed and subjected to F-actin staining using Alexa Fluor 594-conjugated phalloidin (Invitrogen, Carlsbad, CA, USA). Fluorescence signals were visualized using the LSM710 laser scanning microscope (Carl Zeiss, Oberkochen, Germany). Cells in which F-actin staining was concentrated in the direction of TGF-β1 were enumerated in 10 random fields at high magnification, and the proportion among the total number of cells was calculated.

2.11 | Cell shape analysis

Cells were imaged using the BZ-8000 microscope (Keyence, Osaka, Japan). The circularity of 30 cells was assessed using ImageJ. A circularity value of 1.0 indicates a perfect circle, whereas those approaching 0.0 indicate an increasingly elongated polygon.

2.12 | Colony formation assay

KO1, KO2, and EV cells were applied to a pluriStrainer (pluriSelect, Leipzig, Germany). The collected cells were seeded at 4×10^3 per well in 96-well culture plates and cultured for 5 days in Cancer Stem Cell Media Premium (ProMab Biotechnologies, Richmond, CA, USA). Colonies were counted in 5 random fields per well at high magnification.

2.13 | RNA sequencing analysis

Total RNA was extracted from KO1, KO2, and EV HEC-108 cells using the miRNeasy Mini Kit (Qiagen, Hilden, Germany) according to the manufacturer's protocol. cDNA libraries were constructed using the TruSeq Stranded mRNA Sample Prep Kit (Illumina, San Diego, CA, USA) according to the manufacturer's instructions. Sequencing was undertaken on the Illumina HiSeq 2500 platform in 75-base single-end mode. Casava version 1.8.2 software (Illumina) was used for base calling. The sequenced reads were mapped to a human reference genome sequence (hg19) using TopHat version 2.0.13 (http://ccb.jhu.edu/software/tophat/index.shtml), Bowtie2 version 2.2.3 (http://bowtie-bio.sourceforge.net/bowtie2/index.shtml), and SAMtools version 0.1.19 (http://samtools.sourceforge.net/). The fragments per kilobase of exon per million mapped fragments values were calculated using Cuffnorm version. 2.2.1 (http://cole-trapnell-lab.github.io/cufflinks/) to identify upregulated (2.0-fold, $P < .05$) and downregulated (−0.5-fold, $P < .05$) genes.

2.14 | Ingenuity pathway analysis

The gene lists from RNA sequencing were subjected to IPA (Qiagen, https://www.qiagenbioinformatics.com/products/ingenuity-pathway-analysis) to identify pathways that were disturbed by SDPR knockout. In particular, the gene list of KO1 and EV cells, and the list of KO2 and EV cells, were separately subjected to core analysis. Then comparison analysis was carried out using 2 datasets. We focused on the canonical pathway in the results.

2.15 | Effect of ILK inhibition on ALDH1

The effect of ILK inhibition on ALDH1 was evaluated in 2 ways. First, we used ILK inhibitor, OSU-T315 (HY-18676; MedChemExpress, Monmouth Junction, NJ, USA). Empty vector HEC-108 cells (3×10^5) were seeded into 6-well culture plates and incubated for 24 h. Next, 0, 0.1, 0.25, 0.5, 1, 1.5, or 2 μmol/L OSU-T315 was added, and the cells were incubated in DMEM containing 5% FBS for 24 hours. Second, we used siRNA-mediated silencing of ILK. Empty vector HEC-108 cells (1×10^5) seeded into 6-well culture plates were transfected with ILK-targeting siRNA (Silencer Select s7404, s7405, and s7406; Thermo Fisher Scientific) or nontargeting control siRNA (AM4611; Thermo Fisher Scientific) using Lipofectamine RNAiMAX Reagent (Thermo Fisher Scientific) at a final concentration of 50 nmol/L. The sequences of the ILK-targeting siRNA were GCCGUAGUGUAAUGAUUGA (s7404), CGACCCAAAUUUGACAUGA (s7405), and GAAUCACUCUGGAG AGCUA (s7406). The proportion of ALDH-hi cells was determined using the Aldefluor Kit. In ILK knockdown experiments, cells were subjected to the Aldefluor assay 72 hours after siRNA transfection.

2.16 | Intracellular distribution of ILK

KO1, KO2, and EV HEC-108 cells were cultured in a chamber slide (Nunc Lab-Tek II Chamber Slide System; Merck) for 12 hours to allow adherence. Next, the medium was exchanged for DMEM without FBS, and recombinant TGF-β1 protein was added. After incubation for 12 hours, the cells were fixed with 10% formalin. After treating with blocking buffer, the cells were incubated with an anti-ILK1 Ab (1:100). The Tyramide SuperBoost Kit (Thermo Fisher Scientific) was used to amplify the fluorescence signals, which were visualized using the LSM710 microscope. The ImageJ plot profile tool was used to measure pixel intensity (fluorescence) along the lines passing through the center of the cell. The relative quotient was defined as the ratio of the ILK1 signal intensity of the cell cortex to that of the perinuclear region.

2.17 | Statistical analysis

Data are means ± SE. The significance of the differences was determined using Student's *t* test. *P* values <.05 were considered to indicate statistical significance.

3 | RESULTS

3.1 | Expression of SDPR is increased in invasive EC

To assess the relationship between SDPR expression and invasive EC, we undertook immunohistochemical analyses of tissue sections from EC patients (Table 1). Expression of SDPR was higher in G3 cases than G1 or G2 cases, suggesting that SDPR is expressed mainly in poorly differentiated EC (Figure 1A). Regarding prognostic histological factors, lymphatic invasion was significantly correlated with the expression of SDPR (Figure 1B). Thus, high expression of SDPR contributes to the invasiveness of EC.

The MELF histological pattern has similar immunohistochemical characteristics as EMT.[9,10] In this study, the MELF pattern was significantly correlated with the expression of SDPR, suggesting that SDPR expression is related to the EMT (Figure 1C).

3.2 | Serum deprivation-response protein is expressed in EC cells

We assessed SDPR expression in HEC-1B, HEC-108, HEC-116, and SNG-M EC cells. Serum deprivation-response protein expression was detected in all of these cell lines and was highest

TABLE 1 Correlation between the expression of serum deprivation-response protein and histopathological findings in endometrioid carcinoma

	Number of cases	Proportion of positive cases	Standard error	*P* value
Histological grade				
G1	54	0.33	0.064	0.003*
G2	38	0.29	0.074	
G3	34	0.59	0.084	
Myometrial invasion				
<1/2	86	0.35	0.051	0.090
≥1/2	40	0.48	0.079	
Lymphatic invasion				
–	96	0.34	0.048	0.032
+	30	0.53	0.091	
MELF pattern invasion				
–	43	0.26	0.067	0.008
+	11	0.64	0.145	

**P* value when compared between G1-G2 and G3.MELF, microcystic, elongated, and fragmented.
MELF, microcystic, elongated, and fragmented.

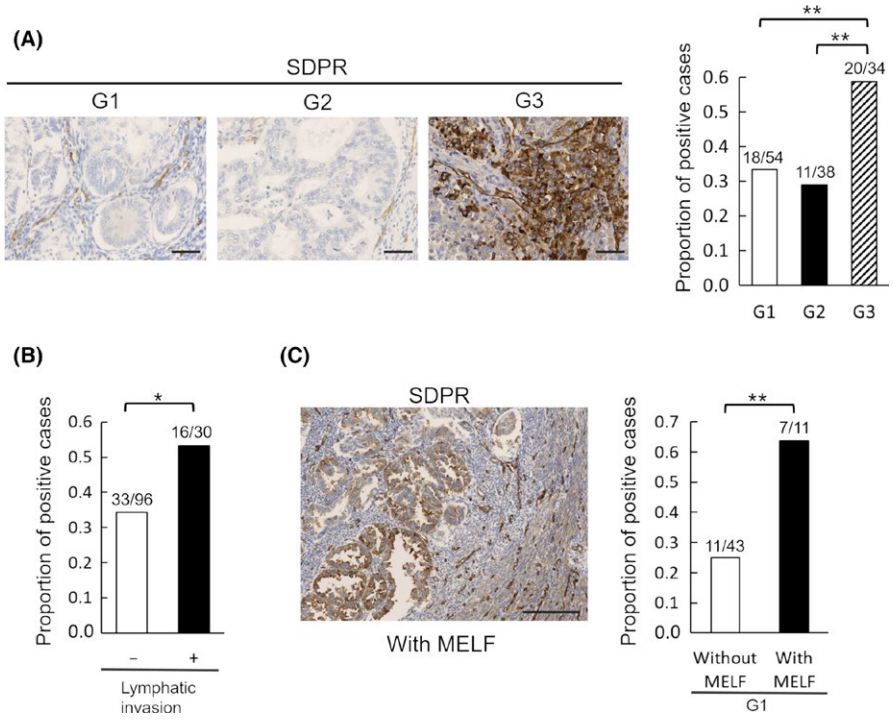

FIGURE 1 Immunohistochemistry of serum deprivation-response protein (SDPR) in clinical endometrioid carcinoma samples. A, Representative immunohistochemically stained images of SDPR and the proportion of positive cases according to histological grade (G1, n = 54; G2, n = 38; G3, n = 34). B, Proportion of positive cases with (n = 30) or without (n = 96) lymphatic invasion. C, Representative immunohistochemically stained image of SDPR with the microcystic, elongated, and fragmented (MELF) pattern and the proportion of positive G1 cases with (n = 11) or without (n = 43) the MELF pattern. Scale bar = 50 μm (A) and 200 μm (C). Student's *t* test: **P* < .05, ***P* < .01

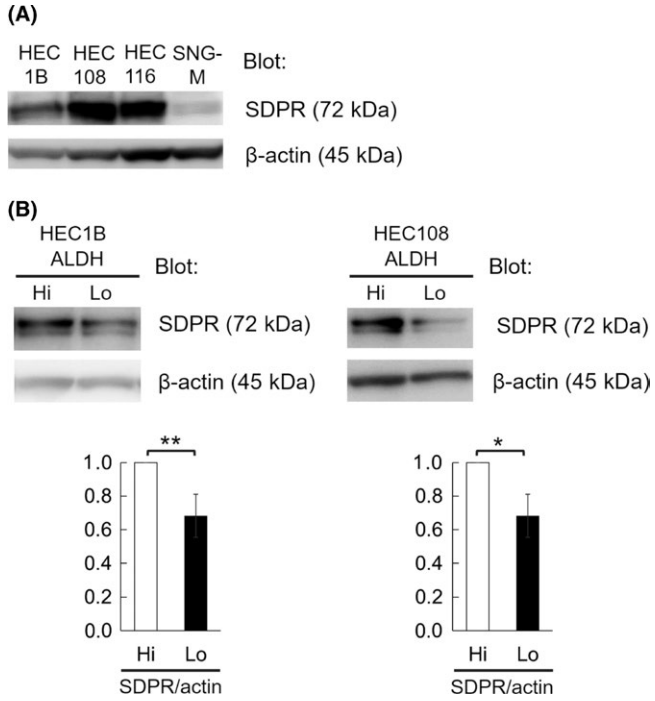

FIGURE 2 Immunoblotting of serum deprivation-response protein (SDPR) in endometrioid carcinoma cells. A, SDPR protein levels in HEC1B, HEC108, HEC116, and SNG-M cells. B, HEC-1B and HEC-108, ALDH-hi cells showed higher levels of SDPR than that of ALDH-lo cells. Equal protein loading was confirmed by quantifying β-actin levels (input control). Data are representative of 3 independent experiments. We quantified the results using ImageJ. SDPR/β-actin quotient of ALDH-hi cells is expressed as 1. The relative quotient of ALDH-lo cells is presented as the ratio to that of ALDH-hi cells. Results are shown as the mean ± SE. Student's *t* test: **P* < .05, ***P* < .01

in HEC-108 (Figure 2A). Thus, we selected HEC-1B, which had been used for shotgun proteomics, and HEC-108. Using the Aldefluor assay, ALDH-hi HEC-1B and HEC-108 cells showed significantly higher expression of SDPR than that of ALDH-lo cells (Figure 2B).

3.3 | Involvement of SDPR in the invasion and migration of EC cells

We constructed an SDPR-knockout HEC-1B and HEC-108 cell line using the CRISPR/Cas9 system to evaluate the function of SDPR (Figure 3A). Knockout of SDPR attenuated the invasion and migration (Figure 3C,D), but not the proliferation (Figure 3B). Thus, SDPR is involved in the invasion and migration, but not proliferation, of EC cells.

3.4 | Involvement of SDPR in formation of lamellipodia

Lamellipodia, in which F-actin accumulates, form at the leading edge of migrating cells.[11] Based on the phenotype of SDPR-knockout cells, we hypothesized that SDPR promotes the formation of lamellipodia. In a chemotaxis assay, SDPR-knockout cells showed impaired formation of lamellipodia towards the chemoattractant compared with control cells (Figure 3E).

3.5 | Effect of SDPR on EMT

The EMT is the process by which a polarized epithelial cell assumes a mesenchymal cell phenotype, including enhanced

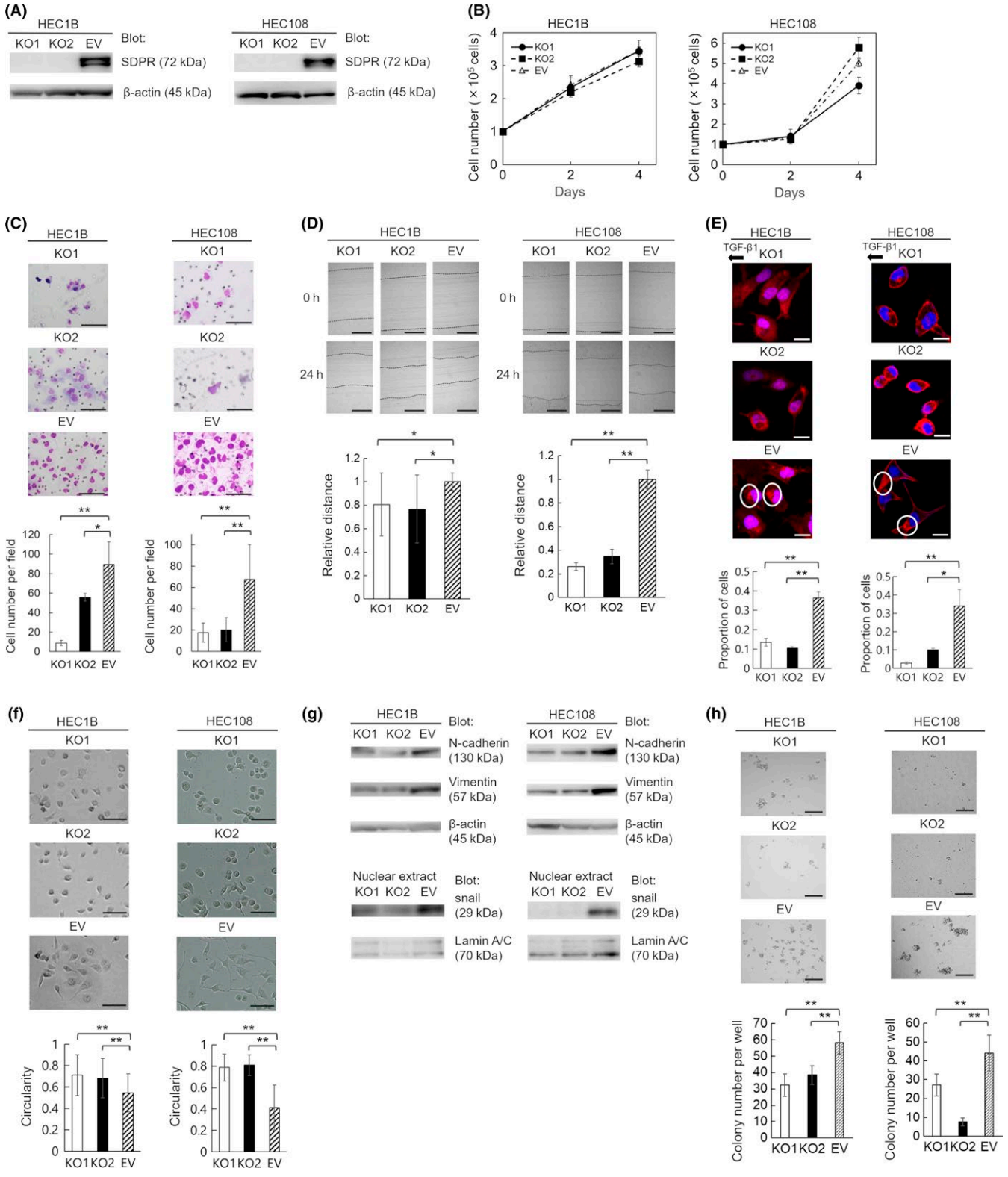

migratory capacity and invasiveness.[12] The SDPR-knockout cells were more rounded than control cells (Figure 3F). As we found SDPR to be related to cell shape, migration, and invasion, we hypothesized that it is also involved in the EMT. During the EMT, the expression of mesenchymal N-cadherin is increased, and master regulators, including snail, twist, and zinc-finger E-box-binding transcription factors, are activated.[13] Immunoblotting indicated that the levels of N-cadherin and vimentin in cell lysates, and that of snail in nuclear extracts, of SDPR-knockout cells were markedly reduced (Figure 3G). Therefore, SDPR promotes the EMT not only in clinical samples but also in cell lines.

FIGURE 3 Generation of serum deprivation-response protein (SDPR)-knockout HEC-1B and HEC-108 cells using the CRISPR/Cas9 system and functional analysis of SDPR. A, Confirmation of loss of SDPR expression in SDPR-knockout cells (KO1 and KO2) by immunoblotting. Equal protein loading was confirmed by quantifying β-actin (input control). EV, control cells. B, Cell proliferation on days 2 and 4. C, Matrigel invasion assay. Representative images of invading KO1, KO2, and EV cells are shown. Invasive cells were counted in 5 random fields per well. D, Wound-healing assay. KO1, KO2, and EV cell layers were wounded with a pipette tip, and migration toward the wounded area was monitored. The distance of migration was calculated by subtracting the width of the wound at 24 h from that at 0 h. The distance of migration of EV cells is expressed as 1. The relative migration distance of KO1 and KO2 cells is presented as the ratio to that of EV cells. E, Chemotaxis assay. Representative images of KO1, KO2, and EV cells; proportion of cells in which F-actin aggregated in the direction of transforming growth factor-β1 (TGF-β1) in 10 random fields. F, Shapes of KO1, KO2, and EV cells. G, Immunoblotting of N-cadherin and vimentin in the cell lysate and snail in the nuclear extracts from KO1, KO2, and EV cells. Equal protein loading was confirmed by quantifying β-actin in cell lysates and lamin A/C in nuclear extracts. H, Colony formation assay. Representative images of colonies of KO1, KO2, and EV cells. Colonies were counted in 5 random fields per well. Data are representative of 3 independent experiments and are shown as means ± SE (B–F, H). Scale bar = 100 μm (C), 200 μm (D), 20 μm (E), 100 μm (F), and 1 mm (H). Student's *t* test: $^{*}P < .05$, $^{**}P < .01$

3.6 | Involvement of SDPR in colony formation by EC cells

Colony formation is a characteristic of stemness. In comparison with control cells, SDPR-knockout cells formed fewer colonies in vitro (Figure 3H). Therefore, SDPR promotes colony formation by EC cells.

3.7 | Serum deprivation-response protein regulates expression of ALDH1

Aldehyde dehydrogenase 1 is related to the tumorigenic potential of EC. Both immunoblotting and Aldefluor assay showed that SDPR knockout significantly reduced the expression of ALDH1 (Figure 4A). Although we previously reported the function of S100A4 or ADSL, which were highly expressed in EC cells with high ALDH1 expression, the depletion of S100A4 or ADSL did not affect the expression of ALDH1. Serum deprivation-response protein is the first protein known to alter the expression of ALDH1 among the isolated proteins previously reported.

3.8 | Effect of SDPR on the ILK signaling pathway

In HEC-108 cells, SDPR expression was higher and the depletion of SDPR affected the ALDH1 expression more strongly than in HEC-1B cells (Figure 4A). Then we used HEC-108 cells and made further analyses. We undertook RNA sequencing of SDPR-knockout and control HEC-108 cells and analyzed canonical pathways impaired in SDPR-knockout cells using IPA. Among the list shown in Table 2, we focused on the ILK signaling pathway. Wickström et al[14] reported that ILK is critical for caveolae formation in mouse keratinocytes. As SDPR is a component of caveolae, we hypothesized that ILK signaling is highly related to SDPR in EC.

In EV HEC-108 cells, ILK-inhibitor OSU-T315 significantly suppressed the expression of ALDH1 and did not affect the expression level of SDPR (Figure 4B). Moreover, we transfected EV HEC-108 cells with 3 individual siRNA duplexes specific for ILK (siILK #1, #2 and #3), or a nontargeting control siRNA (siControl), and confirmed the decrease in ILK1 protein expression in ILK knockdown cells. Then we found that, in ILK knockdown cells, the expression of ALDH1 was severely attenuated and the expression level of SDPR was not affected (Figure 4C). Thus, both SDPR and ILK regulate the expression of ALDH1, and SDPR could function upstream of ILK.

3.9 | Involvement of SDPR in activation of AKT-dependent signaling

Lynch et al[15] reported that ILK regulates AKT Ser473 phosphorylation in COS cells. Therefore, we hypothesized that SDPR promotes AKT phosphorylation by activating ILK signaling. Immunoblotting revealed significantly lower levels of AKT phosphorylation in SDPR-knockout HEC-108 cells (Figure 4D). Therefore, SDPR enhances AKT phosphorylation by activating ILK signaling.

3.10 | Intracellular distribution of ILK1

Immunoblotting showed that ILK1 expression was unaffected by SDPR (Figure 4E). However, immunofluorescence imaging showed that ILK1 was localized at the cell cortex in control HEC-108 cells but was distributed diffusely throughout the cytoplasm of SDPR-knockout HEC-108 cells (Figure 4E). Therefore, the attenuation of ILK signaling by SDPR-knockout might be caused by altered distribution of ILK1.

4 | DISCUSSION

We report herein that SDPR modulates ALDH1 expression in EC cells, as depletion of SDPR markedly attenuated the expression of ALDH1. Previous reports identified some molecules that could affect ALDH1. Matsumoto et al[16] reported that the left-right determination factor (LEFTY) activates ALDH1 in ovarian clear cell carcinoma. Gong et al[17] reported that Nodal upregulates ALDH1 in breast cancer. In contrast, we indicated that Nodal inhibits ALDH1 in EC and lung adenocarcinoma.[18,19] Although we previously reported the function of S100A4 or ADSL, which were highly expressed in EC cells with high ALDH1 expression, the depletion of S100A4 or ADSL did not affect the expression of ALDH1.[3,4] Among the isolated proteins we previously reported, SDPR is the first found to influence the expression of ALDH1.

To analyze the mechanism underlying the effect of SDPR on ALDH1, we undertook RNA sequencing and found that ILK

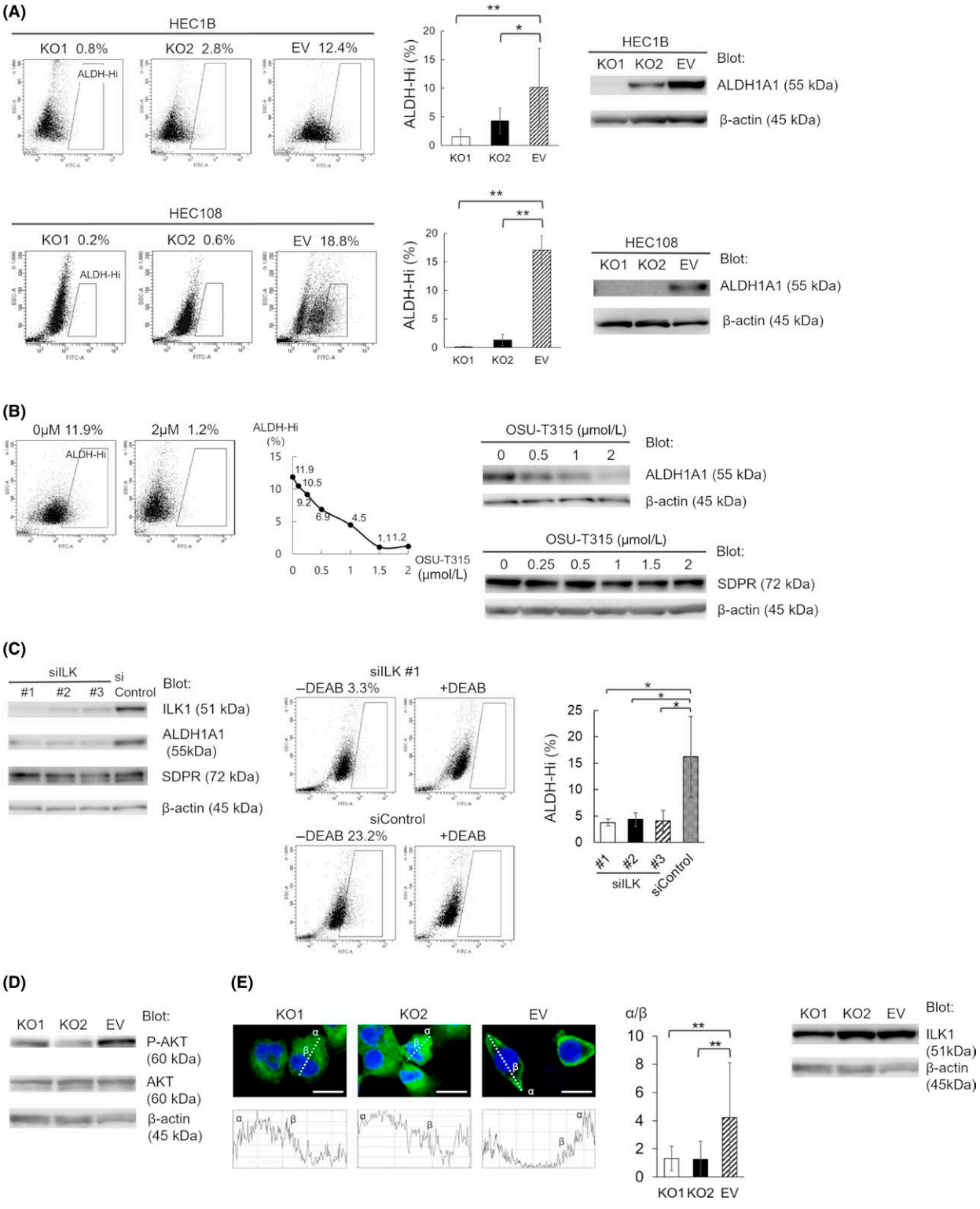

signaling was highly related to SDPR according to IPA. Moreover, the distribution of ILK was related to ILK signaling, as immunofluorescence imaging showed that ILK was distributed diffusely in the cytoplasm of SDPR-knockout cells, but at the cortex in control cells. After forming a ternary complex with the 2 adaptor proteins pinch and parvin, ILK is recruited to focal adhesions in the cell membrane where it activates ILK signaling.[20] Therefore, recruitment of ILK to the cell membrane is essential for ILK signaling. Regarding the relationship between ILK and ALDH1, Hsu et al[21] reported that inhibition of ILK suppresses ALDH1 expression in breast cancer cells; we report a similar phenomenon in EC cells. However, the mechanism by which ILK regulates ALDH1 is unclear. Regarding the relationship between ILK and AKT Ser473 phosphorylation, Lynch et al[15] reported that ILK functions as an adaptor to recruit

FIGURE 4 Serum deprivation-response protein (SDPR) regulates aldehyde dehydrogenase 1 (ALDH1) through integrin-linked kinase (ILK) signaling. A, Proportion of ALDH-hi cells according to Aldefluor staining (left and middle) and the ALDH1A1 protein level (right) in SDPR-knockout KO1, KO2, and empty vector (EV) HEC-1B and HEC-108 cells. Equal protein loading was confirmed by quantifying β-actin (input control). B, Effect of OSU-T315 on the proportion of ALDH-hi cells (left and middle) and the ALDH1A1 and SDPR protein level in EV HEC-108 cells (right). Equal protein loading was confirmed by quantifying β-actin (input control). C, Conformation of ILK knockdown in siILK #1, #2, and #3 EV HEC-108 cells and effect of ILK knockdown on the ALDH1A1 and SDPR protein level (left). Equal protein loading was confirmed by quantifying β-actin (input control). Proportion of ALDH-hi cells in siILK #1, #2, #3, and siControl cells according to Aldefluor staining (middle and right). Dot-blot of Aldefluor assay without inhibitor (left panels), and that with inhibitor (right panels). D, Immunoblotting of AKT and phospho-AKT protein levels in KO1, KO2, and EV HEC-108 cell lysates. Equal protein loading was confirmed by quantifying β-actin (input control). E, Representative images of KO1, KO2, and EV HEC-108 cells in a chamber slide. Cells were fixed and stained with an anti-ILK1 Ab (left 3 pictures). Scale bar = 20 μm. The plot profile along the lines passing through the center of the cell (left 3 graphs). The relative quotient was defined as the ratio of the pixel intensity of the cell cortex (α) to that of the perinuclear region (β) (middle). ILK1 protein levels in KO1, KO2, and EV HEC-108 cell lysates (right) were measured by immunoblotting. Equal protein loading was confirmed by quantifying β-actin (input control). Data are representative of 3 independent experiments and are shown as means ± SE (A,C,E). Student's *t* test: $^{*}P < .05$, $^{**}P < .01$

TABLE 2 List of canonical pathways analyzed by ingenuity pathway analysis (IPA)

Name of canonical pathway	Activation *z*-score[†]
Gα12/13 signaling	−2.496
ILK signaling	**−2.262**
Role of NFAT in regulation of the immune response	−2.082
Glioma invasiveness signaling	−2.058

[†]Top four pathways, with score of less than −2, out of total 121 canonical pathways analyzed by IPA. We took the average of activation *z*-score of serum deprivation-response protein knockout cells (KO1) vs control cells (EV), and KO2 vs EV.
ILK, integrin-linked kinase; NFAT, nuclear factor of activated T-cells.

a Ser473 kinase or phosphatase. Moreover, Chappell et al[22] reported that dysregulation of AKT/mTOR cascades can contribute to proliferation of cancer initiating cells. As ALDH1 is a potential marker of cancer initiating cells, the ILK/ALDH1 pathway can be correlated with the ILK/AKT/mTOR pathway. This warrants further investigation.

It has been reported that SDPR exerts tumor suppressor activity in breast, liver, oral, kidney and prostate cancer.[23–27] Moreover, Ozturk et al[23] reported that SDPR suppresses metastasis of breast cancer by promoting apoptosis of cancer cells; Tian et al[24] showed that SDPR inhibits breast cancer progression by blocking TGF-β signaling. In this study, we found that SDPR is related to tumor progression in EC. In clinical EC specimens, high expression of SDPR was related to enhanced invasiveness (in terms of G3, lymphatic invasion, and MELF). In cell lines, high SDPR expression was correlated with invasion, migration, the EMT, and colony formation. Moreover, data from the Human Protein Atlas (http://www.proteinatlas.org/) show that a high level of SDPR mRNA is correlated with a poor prognosis. We speculate that this is because SDPR-mediated signal activation in caveolae varies according to the type of cancer in question. Indeed, other members of the caveolin and cavin families are involved in tumor suppression and oncogenesis.[8]

Our findings reveal that SDPR modulates the expression of ALDH1 through ILK signaling in EC cells. Moreover, SDPR is associated with several histological characteristics of invasiveness, including MELF. This is, to our knowledge, the first report that SDPR is related to tumor progression.

ACKNOWLEDGMENTS

We thank Ms. Etsuko Maeno, Ms. Takako Sawamura, and Mr. Masaharu Kohara for their technical assistance.

DISCLOSURE

The authors have no conflict of interest.

ORCID

Shinichiro Tahara https://orcid.org/0000-0001-6134-3275

REFERENCES

1. Ginestier C, Hur MH, Charafe-Jauffret E, et al. ALDH1 is a marker of normal and malignant human mammary stem cells and a predictor of poor clinical outcome. *Cell Stem Cell*. 2007;1:555-567.
2. Rahadiani N, Ikeda J, Mamat S, et al. Expression of aldehyde dehydrogenase 1 (ALDH1) in endometrioid adenocarcinoma and its clinical implications. *Cancer Sci*. 2011;102:903-908.
3. Tahara S, Nojima S, Ohshima K, et al. S100A4 accelerates the proliferation and invasion of endometrioid carcinoma and is associated with the "MELF" pattern. *Cancer Sci*. 2016;107:1345-1352.
4. Park H, Ohshima K, Nojima S, et al. Adenylosuccinate lyase enhances aggressiveness of endometrial cancer by increasing killer cell lectin-like receptor C3 expression by fumarate. *Lab Invest*. 2018;98:449-461.
5. Parton RG, del Pozo MA. Caveolae as plasma membrane sensors, protectors and organizers. *Nat Rev Mol Cell Biol*. 2013;14:98-112.
6. Anderson RG. The caveolae membrane system. *Annu Rev Biochem*. 1998;67:199-225.
7. Hansen CG, Bright NA, Howard G, et al. SDPR induces membrane curvature and functions in the formation of caveolae. *Nat Cell Biol*. 2009;11:807-814.

8. Gupta R, Toufaily C, Annabi B. Caveolin and cavin family members: dual roles in cancer. *Biochimie*. 2014;107:188-202.
9. Murray SK, Young RH, Scully RE. Unusual epithelial and stromal changes in myoinvasive endometrioid adenocarcinoma: a study of their frequency, associated diagnostic problems, and prognostic significance. *Int J Gynecol Pathol*. 2003;22:324-333.
10. Stewart CJ, Little L. Immunophenotypic features of MELF pattern invasion in endometrial adenocarcinoma: evidence for epithelial-mesenchymal transition. *Histopathology*. 2009;55:91-101.
11. Koestler SA, Rottner K, Lai F, et al. F- and G-actin concentrations in lamellipodia of moving cells. *PLoS ONE*. 2009;4:e4810.
12. Kalluri R, Weinberg RA. The basics of epithelial-mesenchymal transition. *J Clin Invest*. 2009;119:1420-1428.
13. Lamouille S, Xu J, Derynck R. Molecular mechanisms of epithelial-mesenchymal transition. *Nat Rev Mol Cell Biol*. 2014;15:178-196.
14. Wickström SA, Lange A, Hess MW, et al. Integrin-linked kinase controls microtubule dynamics required for plasma membrane targeting of caveolae. *Dev Cell*. 2010;19:574-588.
15. Lynch DK, Ellis CA, Edwards PA, et al. Integrin-linked kinase regulates phosphorylation of serine 473 of protein kinase B by an indirect mechanism. *Oncogene*. 1999;18:8024-8032.
16. Matsumoto T, Yokoi A, Hashimura M, et al. TGF-β-mediated LEFTY/Akt/GSK-3β/Snail axis modulates epithelial-mesenchymal transition and cancer stem cell properties in ovarian clear cell carcinomas. *Mol Carcinog*. 2018;57:957-967.
17. Gong W, Sun B, Sun H, et al. Nodal signaling activates the Smad2/3 pathway to regulate stem cell-like properties in breast cancer cells. *Am J Cancer Res*. 2017;7:503-517.
18. Wang Y, Jiang Y, Tian T, et al. Inhibitory effect of Nodal on the expression of aldehyde dehydrogenase 1 in endometrioid adenocarcinoma of uterus. *Biochem Biophys Res Commun*. 2013;440:731-736.
19. Jiang Y, Li H, Wang Y, et al. ALDH enzyme activity is regulated by Nodal and histamine in the A549 cell line. *Oncol Lett*. 2017;14:6955-6961.
20. Widmaier M, Rognoni E, Radovanac K, et al. Integrin-linked kinase at a glance. *J Cell Sci*. 2012;125:1839-1843.
21. Hsu EC, Kulp SK, Huang HL, et al. Integrin-linked kinase as a novel molecular switch of the IL-6-NF-κB signaling loop in breast cancer. *Carcinogenesis*. 2016;37:430-442.
22. Chappell WH, Steelman LS, Long JM, et al. Ras/Raf/MEK/ERK and PI3K/PTEN/Akt/mTOR inhibitors: rationale and importance to inhibiting these pathways in human health. *Oncotarget*. 2011;2:135-164.
23. Ozturk S, Papageorgis P, Wong CK, et al. SDPR functions as a metastasis suppressor in breast cancer by promoting apoptosis. *Proc Natl Acad Sci USA*. 2016;113:638-643.
24. Tian Y, Yu Y, Hou LK, et al. Serum deprivation response inhibits breast cancer progression by blocking transforming growth factor-β signaling. *Cancer Sci*. 2016;107:274-280.
25. Jing W, Luo P, Zhu M, et al. Prognostic and diagnostic significance of SDPR-Cavin-2 in hepatocellular carcinoma. *Cell Physiol Biochem*. 2016;39:950-960.
26. Unozawa M, Kasamatsu A, Higo M, et al. Cavin-2 in oral cancer: a potential predictor for tumor progression. *Mol Carcinog*. 2016;55:1037-1047.
27. Li X, Jia Z, Shen Y, et al. Coordinate suppression of Sdpr and Fhl1 expression in tumors of the breast, kidney, and prostate. *Cancer Sci*. 2008;99:1326-1333.

How to cite this article: Tahara S, Nojima S, Ohshima K, et al. Serum deprivation-response protein regulates aldehyde dehydrogenase 1 through integrin-linked kinase signaling in endometrioid carcinoma cells. *Cancer Sci*. 2019;110:1804–1813. https://doi.org/10.1111/cas.14007